Tata H (2024)
Nova Geodesia 4(2):180
Research Article

Insight into the Global Gravity Models for Free-Air Gravity Estimation using Land Gravity Data

Herbert TATA

Federal University of Technology, Department of Surveying and Geoinformatics, Akure, Ondo State, Nigeria; htata@futa.edu.ng

Abstract

Gravity anomalies are used for the interpretation of the structures which are beneath the Earth. The availability of gravity anomalies at the early stage of exploration activities makes determining characteristics, forms and location properties beneath the Earth's crust possible. Different GGMs have different accuracies due to factors such as differences in sources of data and the mode of their formulation. It is essential to know the efficiency of models over an area before being used for serious activity over the area. This research evaluated gravity anomaly derived from Global Gravity Models to determine the best-fit model over Akure City, Nigeria, by accessing ten gravitational models over twenty-three geodetic control points. Free-Air was the Gravity field model, calculated through the ten Global Gravity field Models over the study area. The computations of the anomalies were done at the International Centre for Global Earth Models (ICGEM). Terrestrial gravity anomaly data acquired was the standard against the ten model-based gravity anomalies using a coefficient of correlation and T-test to determine the best models over the area. Based on correlation analysis, SGG_UGM_2 has a value of 0.5995, and EGM2008 was 0.5973, respectively. The two models are the best fit for the study area. Based on the T-test for Free-Air anomaly data, EGM2008 and GECO have no significant difference from the terrestrial gravity models having P-values of 0.0393 mgal and 0.0146 mgal, respectively. This research, therefore, underscores the significance of adopting the best-fit model over the study area.

Keywords: Free-Air Gravity; Global Gravity Models; Terrestrial gravity anomaly

Introduction

Free-Air anomaly is the difference between the observed gravity and the theoretical gravity at sea level, plus a Free-Air coefficient based on the height of the measurement station, which is used to compute the mass excesses and deficits within the Earth. It is often thought that the significant Free-Air gravity irregularities and heat flow irregularities on the oceanic ridges are the surface manifestations of the high temperatures and flow in the mantle (McKenzie, 1967). Gravity anomalies are used for the interpretation of the structures which are beneath the Earth. With the gravity anomalies provided at the early stage of the exploration program, it will be possible to determine the properties, forms, and locations of certain properties in the subsurface. The earth models remove the anomalies and inconsistencies in the gravity data. This is possible when the sources of the

Received: 26 Mar 2024. Received in revised form: 19 May 2024. Accepted: 30 May 2023. Published online: 30 May 2024.

anomalies are known, such as the rotation of the Earth, the distance from the geocentric, topographic relief, tidal inconsistency and gravity meter malfunction (Yılmaz and Kozlu, 2018).

This research addresses the following questions: what are the most suitable recent Global Gravitational Models and high-degree Global Gravity Models for accurately determining gravity anomalies in Akure? What is the accuracy level achieved by the selected high-degree Global Gravity Models and recent Global Gravitational Models (lower degree) in estimating gravity anomalies in Akure? Can the recent Global Gravitational Models with lower degrees produce gravity anomaly values comparable to or better than those obtained from high-degree Global Gravity Models?

The study will significantly enhance our understanding of the practical implications of Global Gravity Models for estimating Free-Air gravity anomalies using land gravity data and underscore their relevance across various sectors. This will go a long way by improving geodetic surveying, particularly for engineering and construction projects where precise measurements are essential. Accurate gravity anomaly estimation can aid in resource exploration, such as identifying potential mineral deposits or groundwater resources. By leveraging Global Gravity Models, researchers and industries can make informed decisions regarding resource allocation and extraction strategies. The insights gained from the research will contribute to geophysical studies by understanding the subsurface geological structures and tectonic processes. This can further aid in assessing seismic hazards, groundwater movement, and other geological phenomena.

In this research, ten gravitational models were acquired from ICGEM and analysed over twenty-three geodetic stations upon which gravity anomalies were obtained. The main component of gravity anomaly in this research is the Free-Air anomaly. Geodetic coordinates and observed Free-Air anomalies were obtained from (Tata and Ono, 2018). The anomalies of the Free-Air (satellite-based) were acquired from the International Digital Elevation Model Service (ICGEM) site.

This research aims to assess the accuracy of Global Gravity Models for Free-Air anomaly estimation using land gravity data in Akure City, Nigeria, to determine the best-fit model over Akure City, Nigeria. A feasible Global model recommendable for gravity anomaly modelling in geodetic applications will be evaluated.

Gravity, Terrestrial Gravity Data and GGMs

Gravity anomaly

In the geophysical context, anomalous gravity is computed by subtracting a predicted or modelled gravity value for a point P from the measured (observed) gravity at that point. This anomalous gravity quantity is technically referred to as a gravity disturbance (Hackney and Featherstone, 2003). Gravity anomaly can be expressed as:

$$\Delta g_p = g_p - y_p \quad (1)$$

Where:

Δg_p signifies the observed gravity anomaly at a particular location, labelled as p. Meanwhile, g_p denotes the actual measured gravitational force at that identical location or point, and y_p stands for the expected or theoretical gravitational force expected at the same location or point.

Free-Air correction

The Free-Air reduction' is used to partly downward or upward-continue observed gravity to the geoid using the vertical gradient of normal gravity as an approximation (Hackney and Featherstone, 2003). The elevation of the point where each gravity measurement is determined should always be reduced to a reference datum to compare the complete profile. This is called the Free-Air correction (F), and when combined with the latitude, it leaves the Free-Air anomaly (Yilmaz and Yilmaz, 2018). The Free-Air reduction accounts for gravity observations not made on the vertical datum surface. It is essentially a correction to the observed gravity for the inverse distance-squared decay of gravity on moving away from the Earth (Featherstone and Dentith, 2010). Following Yilmaz *et al.* (2018), the linear approximation of Free-Air correction as:

$$F = -\frac{\partial \gamma}{\partial R} H \approx 0.3086H \quad (2)$$

Based on Yilmaz *et al.* (2018), in Eq. (2), the Free-Air correction, denoted as F, accounts for gravitational adjustments. R is the radius of the spherical Earth and H is the height or altitude above the reference surface, often the Earth's surface. The theoretical value of the normal gravity at that point predicted from a reference ellipsoid is denoted as γ. Considering the oblate shape, the derived second-order approximation of Free-Air gravity anomaly (Δg_{FA}), is expressed in Equation 3:

$$\Delta g_{FA} = g_P + F - \gamma \quad (3)$$

Terrestrial gravity data

Terrestrial gravity data invalidate data produced by GGMs. The terrestrial data used in this is secondary data. Gravity anomaly for each of the observed points within the study area was computed using the international gravity formula of geodetic system 1930 for normal computation of equation (4):

$$\gamma o = 9.78049(1 + 0.0052884 sin^2\varphi - 0.0000059 sin^2 2\varphi) m.s^{-2} \quad (4)$$

Based on Tata and Matthew (2018), the variable φ is the latitude. The gravity anomaly was computed by subtracting the normal gravity at the reference ellipsoid from the point gravity at the geoid, as shown in equation (5):

$$\Delta g = g_p - \gamma_Q \quad (5)$$

where Δg = gravity anomaly, g_p= gravity at the geoid, γ_Q= normal gravity at the reference ellipsoid. Terrestrial gravity is costly because of the processes and instruments used in the observation. However, the results are reliable data used to determine geoid and as a reference to some other observational activities of gravity.

Global Gravitational Model

One of the main objectives of geodesy is to determine the Global Gravitational field of the Earth. Since the 1960s, gravity data from ships, land, and satellites have been used to estimate the Earth's true gravitational potential, as have spherical harmonic-derived marine gravity anomalies (Barthelmes, 2013). "GM" refers to the spherical harmonic coefficients that express the Earth's gravitational potential in space. Knowledge of the Earth's structure, composition, interior, and fluid envelope is provided by GMs.

Knowledge of the Earth's structure, composition, interior, and fluid envelope is provided by GMs. GMs can calculate all relevant gravity field functionals. The two main categories of GMs are satellite-only and integrated models. In contrast to the combined models, which also use terrestrial gravity measurements (over the continents) and altimetry measurements (over the oceans), the satellite-only models are generated solely using satellite observations (Barthelmes, 2014). The following equation can be used to express the gravity anomaly (g) through spherical harmonic expansion (Barthelmes, 2013).

$$\Delta g(r, \lambda, \varphi) = \frac{GM}{r^2} \sum_{n=2}^{N_{max}} \left(\frac{R}{r}\right)^n (N-1) \sum_{m=0}^{n} \bar{P}_{nm}(\sin\varphi) [\Delta \bar{C}_{nm} \cos m\lambda + \Delta \bar{S}_{nm} \sin m\lambda] \quad (6)$$

The notations are: (r, λ, φ); radius, longitude, and latitude of the computation point, G; gravitational constant, M; the mass of the Earth, R; reference radius of the Earth, ℓ, m; degree, order of spherical harmonics, Pλm; Legendre functions (fully normalised), Cλm, S λm; Stokes' coefficients (fully normalised). The determination of the Earth's gravitational field has advanced significantly due to the launches of CHAMP, GRACE, and GOCE. Thus, the technological and scientific developments in artificial satellite techniques and calculation algorithms resulted in the release of high-degree combined GMs (Yilmaz *et al.*, 2017).

Global Gravitational Models (GGMs) approximate the external gravitational potential of an attracting body such as the Earth (Apeh *et al.*, 2018; Apeh and Tenzer, 2022). Five high resolutions and five low resolutions were adopted in the research. Further, five combined satellite-based Gravity data, Altimetry data models, four satellite-based models, and one combined gravity and satellite-based model were used. The characteristics of the GGMs used in this research are shown in Table 1 and Table 2.

ICGEM (International Centre for Global Earth Models)

ICGEM is one of five services coordinated by the International Gravity Field Service (IGFS) of the International Association of Geodesy (IAG). ICGEM (*http://icgem.gfz-potsdam.de/home*) is dedicated to collecting and archiving such models and making them available to users on a web-based platform.

Materials and Methods

Study Area

The study area is within the Akure South metropolis Figure 1. The geographic location is approximately between latitudes 07˚15′N to 07˚30′N and between longitudes 05˚15′E to 05˚25′E. Temperature ranges between 22°C and 30°C coupled with high humidity. Akure is about 350 metres above mean sea level and is dominated by chains of rugged hills and rock formations with low-lying flood plains in between (Olujide, 2018). The topography is gently undulating, consisting of gravel, lateritic soil, alluvial soil, clay and top-soil and low-lying outcrops at the lowland area (NPC, 2007).

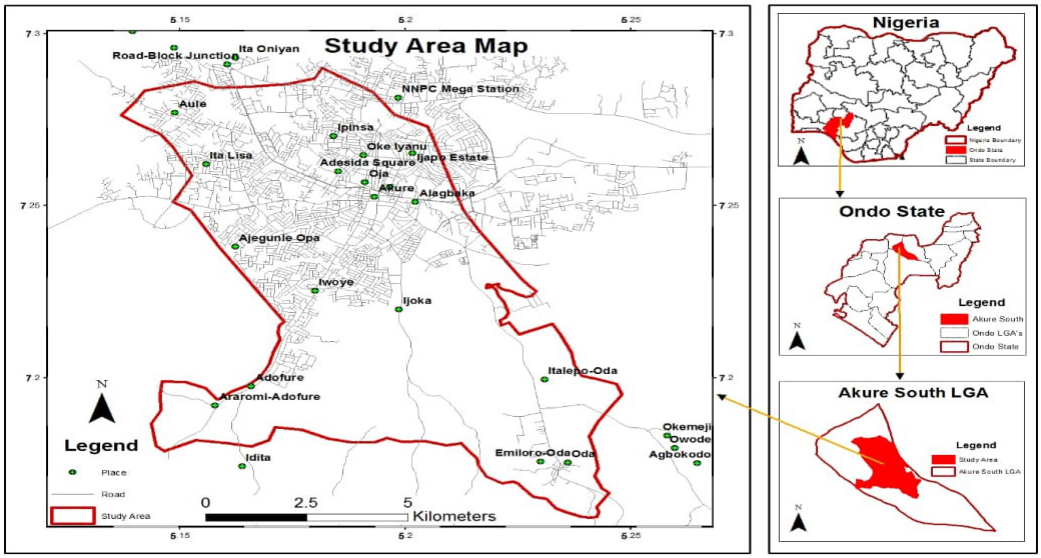

Figure 1. Showing a map of the study area (Tata and Matthew, 2018)

Methods

Ten gravitational models were acquired and analyzed over twenty-three (23) geodetic stations upon which gravity anomalies were obtained. The main component of gravity anomaly in this research is the free-air. Geodetic coordinates and observed Free-Air anomalies were acquired from an existing research work (secondary data). The anomalies of the Free-Air were acquired from the International Digital Elevation Model Service (ICGEM) site. The anomalies were extracted from the ten models serving the geodetic coordinates in CSV format into the site to generate the anomalies computed from the calculation service provided section within the site. The anomalies from the models were acquired in their highest resolution. The spatial wavelength and resolution of the parameters computed from all global field models were directly linked to the maximum degree and the order of expansion. The parameters i.e. spatial resolution, spatial wavelength, reference system (WGS 84), and the earth's equatorial radius were kept fixed throughout the data acquisition. The Free-Air anomaly is obtained from the spherical approximation of the gravity anomaly from Eq. (7): For the statistical analysis, the pooled standard deviation (s_p) was computed using equation 8 while equation 9 was used in carrying out the T-test. The Pearson correlation coefficient was used in measuring the strength and the direction of the linear relationship that axis between the variable's equation 10.

$$\Delta g(\lambda,\phi) \approx \Delta g_{sa}(\lambda,\phi) = -\frac{\partial T^c}{\partial r}\Big|_{h=0} - \frac{2}{r(\phi)} T^c(0,\lambda,\phi) \quad (7)$$

where: r = r(ϕ) is the disturbance to the centre of the coordinate system (spherical coordinate) of a point on the ellipsoid, Δg is gravity anomaly, Δg_{sa} is the spherical approximation and T^c is the disturbing potential.

$$S_p = \sqrt{\frac{(n_1-1)s_1{}^2+(n_1-1)s_1{}^2}{n_1+n_2-2}} \quad (8)$$

where:

n_1 and n_2 are the sample sizes of the variables, and s_1 and s_2 are the standard deviations of the variables.

$$t = \frac{\bar{X}_1 - \bar{X}_2}{s_p\sqrt{\frac{1}{n_1}+\frac{1}{n_2}}} \quad (9)$$

where:

$\bar{X}_1$, $\bar{X}_2$ are the sample means of the variables, s_p is the pooled standard deviation, and n_1, n_2 are the sample sizes of the variables

$$r = \frac{\sum(X_i-\bar{X})(Y_i-\bar{Y})}{\sqrt{\sum(x_i-\bar{X})^2}\sqrt{\sum(y_i-\bar{Y})^2}} \quad (10)$$

where:

r is the Pearson correlation coefficient, X_i, and Y_i are the individual points and $\bar{X}$, $\bar{Y}$ are the means of the X and Y.

Table 1. Five High-Degree Global Gravity Models

No	Name of Model	Degree	Year	Data Source	Reference
1	XGM2019e_2159	2190, 5540, 760	2019	A, G, S (GOCO06s), T	Zingerle *et al.* (2019)
2	GECO	2190	2015	EGM2008, S (Goce)	Gilardoni *et al.* (2016)
3	EIGEN-6C2	2190	2014	EGM2008, S (Goce)	Gilardoni *et al.* (2016)
4	SGG-UGM-2	2190	2020	(A, EGM2008, Grace), S (Goce)	Liang *et al.* (2020)
5	EGM2008	2190	2008	A, G, S (Grace)	Pavlis *et al.* (2012)

Source: *http://icgem.gfz-potsdam.de/tom_longtime*, 2020

Table 2. Five Recent Global Gravity Models

No	Name of Model	Year	Degree	Source of Data	Reference
1	GO_CONS_GCF_2_TIM_R6	2019	300	G (Polar), S(Goce)	Zingerle *et al.* (2019)
2	ITSG-Grace2018s	2019	200	S (Grace)	Mayer-Gürr *et al.* (2018)
3	EIGEN-GRGS.RL04.MEAN-FIELD	2019	300	S	Lemoine *et al.* (2019)
4	GOCO06s	2019	300	S	Kvas *et al.* (2019)
5	GO_CONS_GCF_2_TIM_R6	2019	300	S (GOCE)	Brockmann *et al.* (2014)

Source: *http://icgem.gfz-potsdam.de/tom_longtime*, 2020

Global Gravity Models

Based on the scope of this study's research, these models can be divided into two categories. First, we have five of the most recent GGMs that were launched in 2019. Next, we have the GGMs with high degrees. Table 2 lists the five high-degree global gravity models along with their altimetry (A) and topography (T) values. More specifically, S and T stand for ground data (such as terrestrial, ship-borne, and aerial measurements) and satellite data (such as GRACE, GOCE, and LAGEOS).

Results

Statistical Results

Each row of Table 3 shows the result of a specific test comparing the terrestrial Free-Air anomaly with one of the models. The null hypotheses and alternative hypotheses for the tests are of the form:

$$H_{1i} = H_o \quad vs \quad H_{1i} \neq H_o \tag{8}$$

where H_0 represents the mean of the terrestrial Free-Air anomaly and H_{1i} the mean of the model being compared to the terrestrial Free-Air anomaly.

Table 3. The result of the observations obtained from ten models to that of the Terrestrial Free-Air model

Model	Mean (mgal)	Std. Err (mgal)	Std. dev. (mgal)	95% Conf. Interval (mgal)		T (mgal)	P-value (mgal)
EGM2008	-1.803556	0.8229498	3.946729	-3.51025	-0.0968627	-2.1916	0.0393
EIGEN6c4	5.469787	0.8329006	3.994451	3.742457	7.197117	6.5672	0.0000
GECO	2.210339	0.8334643	3.997155	0.4818402	3.938839	2.6520	0.0146
SGG_UGM_2	5.032043	0.8274182	3.968158	3.316083	6.748004	6.748004	0.0000
XGM2019e_2159	2.715883	0.8558381	4.104456	0.9409832	4.490783	3.1734	0.0044
EIGEN-GRGS.RL04. MEAN-FIELD	14.06128	0.9346207	4.482283	12.123	15.99957	15.0449	0.0000
GOCO06s	13.97704	0.9362127	4.489918	12.03545	15.91863	14.9293	0.0000
ITSG-Grace2018s	17.98267	0.8415972	4.036158	16.23731	19.72804	21.3673	0.0000
GO_CONS_GCF_2_DIR_R6	13.65817	0.9233025	4.428003	11.74336	15.57298	14.7927	0.0000
GO_CONS_GCF_2_TIM_R6	13.937	0.9345104	4.481754	11.99894	15.87506	14.9137	0.0000

The results show that all the models are significantly different from the Terrestrial Free-Air anomaly at 0.05 level of significance, but the EGM2008 and GECO are not significantly different from the Terrestrial Free-Air anomaly at 0.01 level of significance. The P-values of these models, EGM2008 and GECO, are given respectively as 0.0393 and 0.0146, which are all greater than 0.01 significance level.

Correlation Analysis

The correlation analysis results, shown in Table 4, measure the relationship between 10 different models with terrestrial Free-Air anomalies. All models demonstrate a strong correlation with terrestrial data. With a correlation value of 0.5995, the SGG_UGM_2 model indicated a strong correlation with terrestrial Free-Air anomalies. This is followed by the EGM2008 model, which has a correlation value of 0.5973.

Table 4. Correlation analysis between the observations from the ten GGMs and the observed gravity data (Free-Air)

Model	Free-Air (mgal)
EGM2008	0.5973
EIGEN6c4	0.5942
GECO	0.5969
SGG_UGM_2	0.5995
XGM2019e_2159	0.5805
EIGEN-GRGS.RL04.MEAN-FIELD	0.5420
GOCO06s	0.5609
ITSG-Grace2018s	0.5751
GO_CONS_GCF_2_DIR_R6	0.5778
GO_CONS_GCF_2_TIM_R6	0.5613

These two models can be considered the most preferred for adoption when requiring high precision in representing terrestrial gravity anomalies. Furthermore, EIGEN-GRGS.RL04.MEAN-FIELD model shows the lowest correlation value of 0.5420.

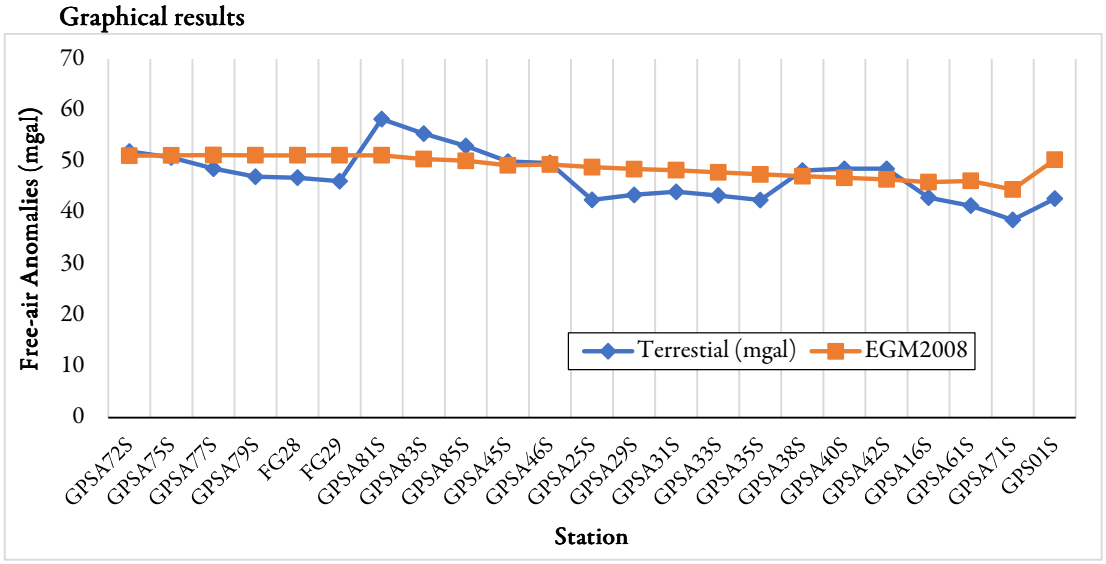

Figure 2. Changes in terrestrial with Egm2008 Free-Air anomaly

It is worth observing in Figure 2 that the terrestrial (mgal) increases slightly with EGM2008 at the rate of 1.384679539. For instance, at the stations GPSA81S and GPS01S, the optimal difference was observed and estimated as 7.0763 and 7.592.

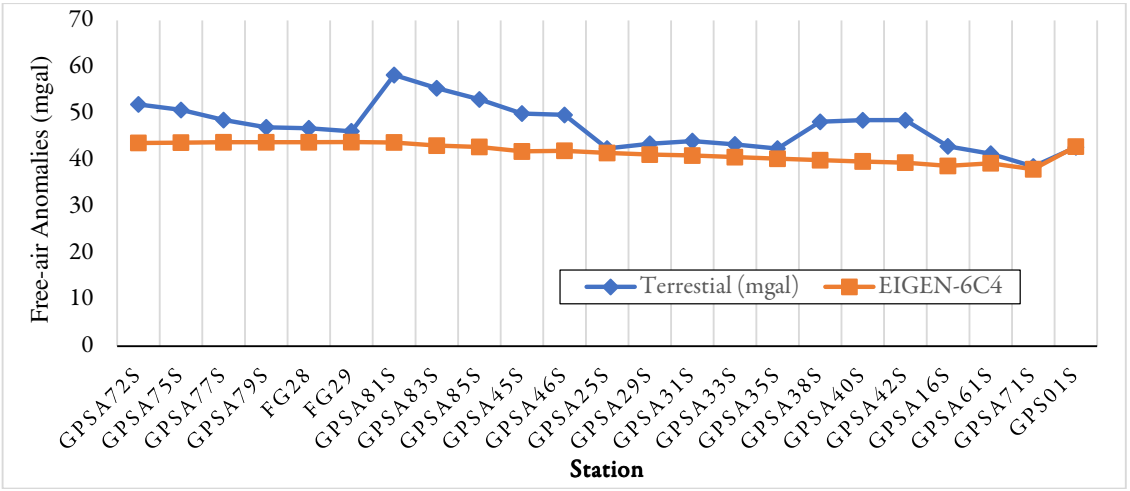

Figure 3. Changes in terrestrial with EIGEN-6C4 Free-Air anomaly

In Figure 3, the positive increase in the Terrestrial (mgal) with EIGEN-6C4 was estimated as 1.508296987. There exists a significant difference at the station GPSA81S. This is true because the terrestrial (mgal) is 58.291, while the EIGEN-6C4 is 43.7817.

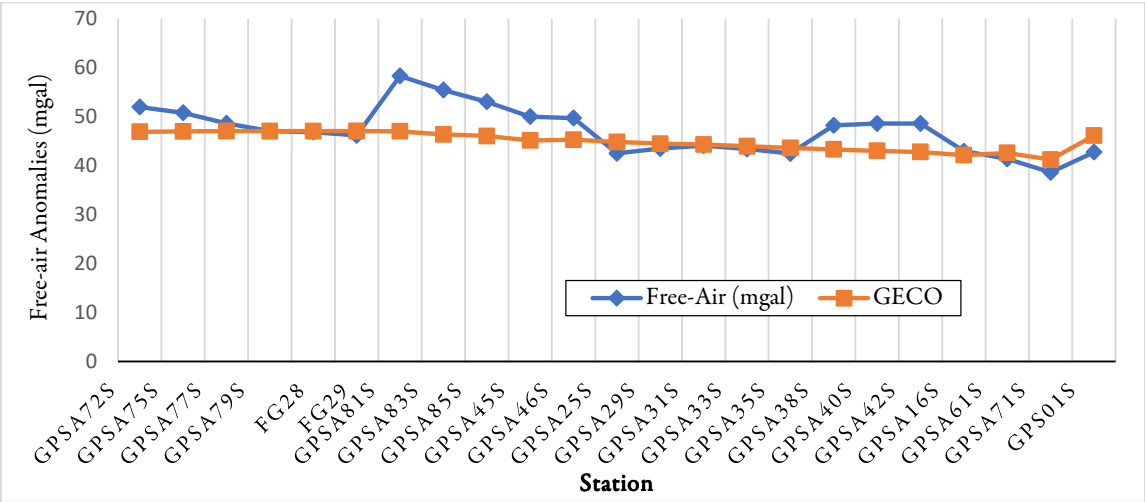

Figure 4. Changes in the terrestrial with GECO Free-Air Anomaly

For the case of Free-Air (mgal) against GECO, the rate of changes between both variables when Free-Air (mgal) depends on GECO increases at the rate of 1.544717219. The most significant difference between the Free-Air (mgal) and GECO manifests at the station GPSA81S.

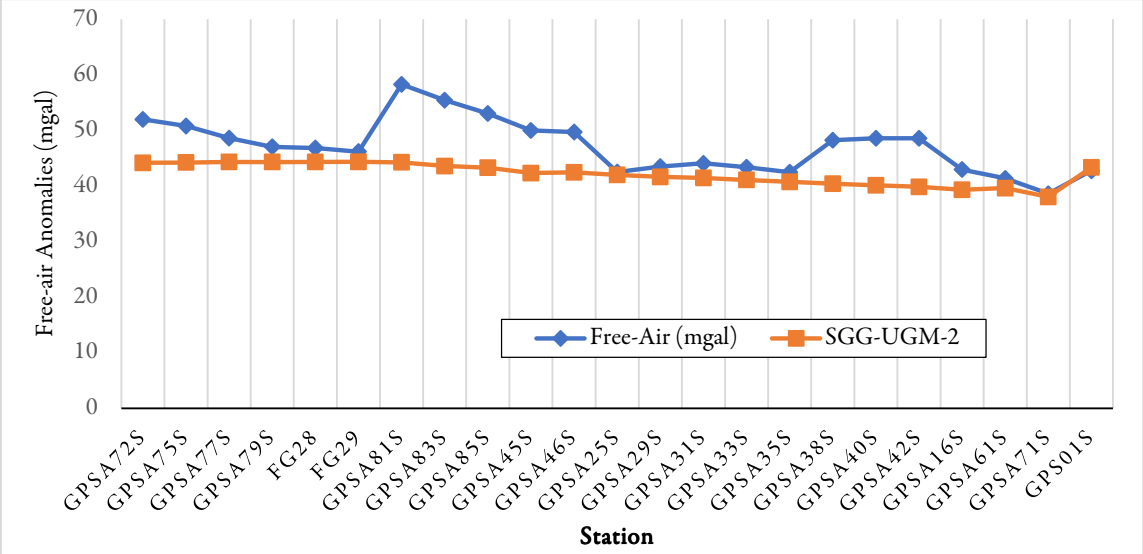

Figure 5. Changes between the terrestrial with SGG-UGM-2 Free-Air anomaly

Figure 5 was further examined, and it was discovered that the Free-Air (mgal) increases with SGG-UGM-2 at the rate of 1.47691504.

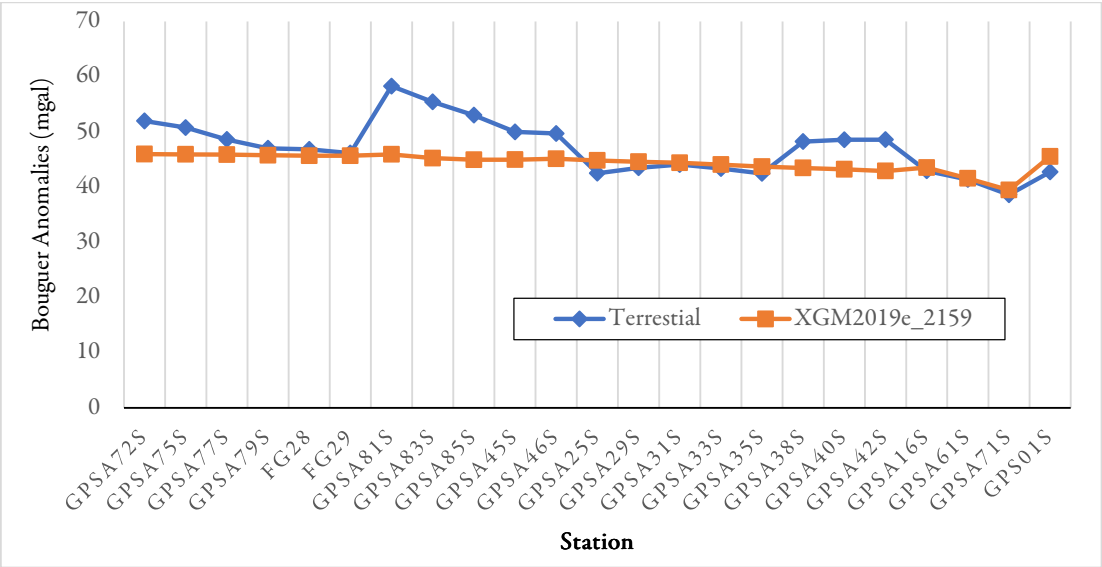

Figure 6. Changes in the terrestrial with XGM2019e_2159 Free-Air anomaly

As seen in Figure 6, Free-Air (mgal) increases with XGM2019e_2159 at 1.755807928.

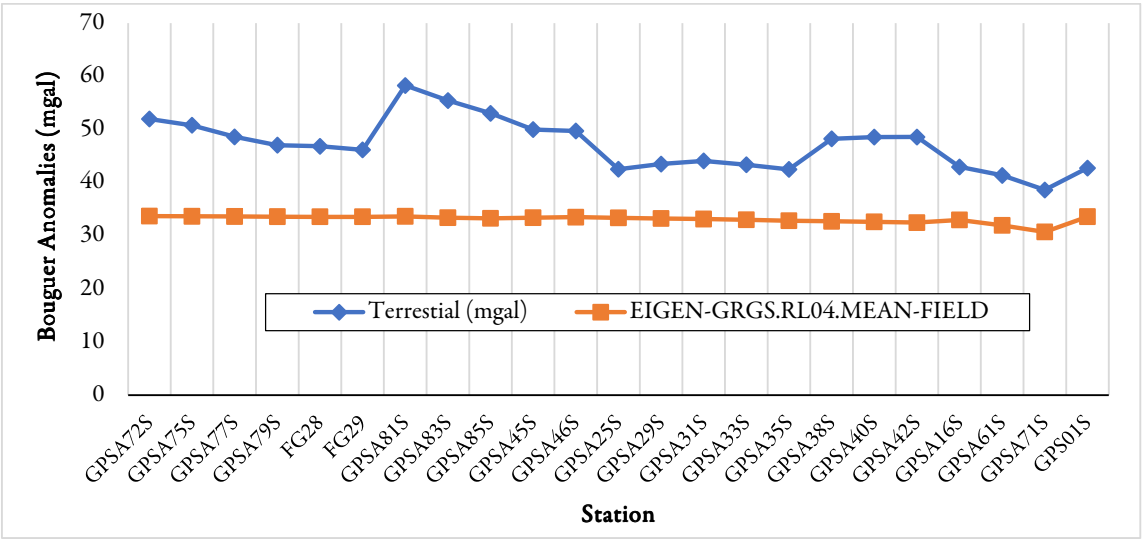

Figure 7. Changes in the terrestrial with EIGEN-GRGS.RL04.MEAN-FIELD Free-Air anomaly

In Figure 7, the terrestrial (mgal) changes with EIGEN-GRGS.RL04.MEAN-FIELD at the rate of 3.779392218.

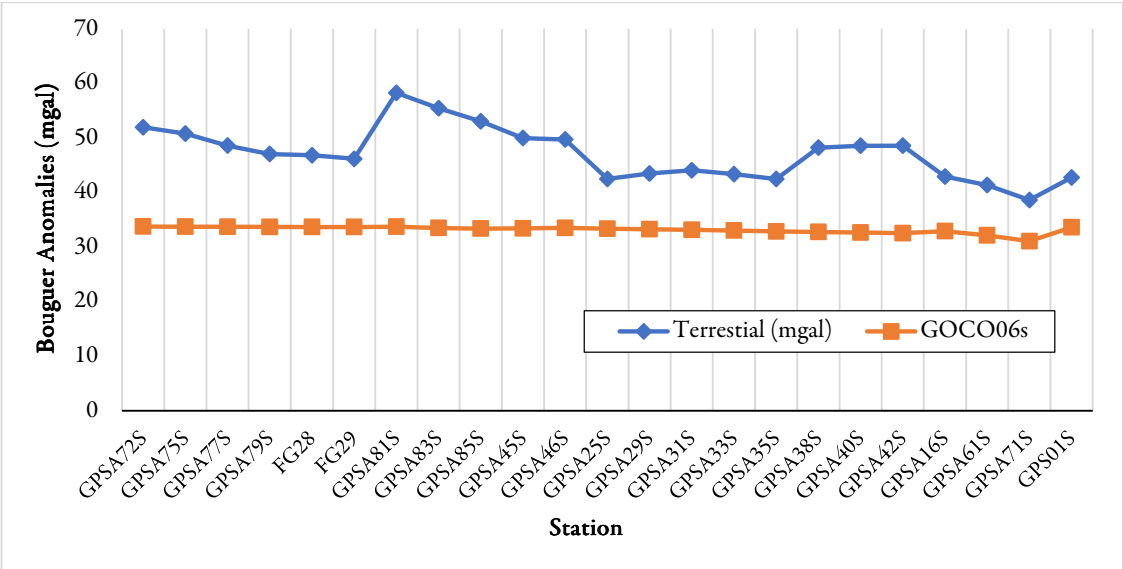

Figure 8. Changes in the terrestrial with GOCO06S Free-Air anomaly

Figure 8, was further examined using the linear slope regression through the data points of terrestrial (mgal) and GOCO06s.

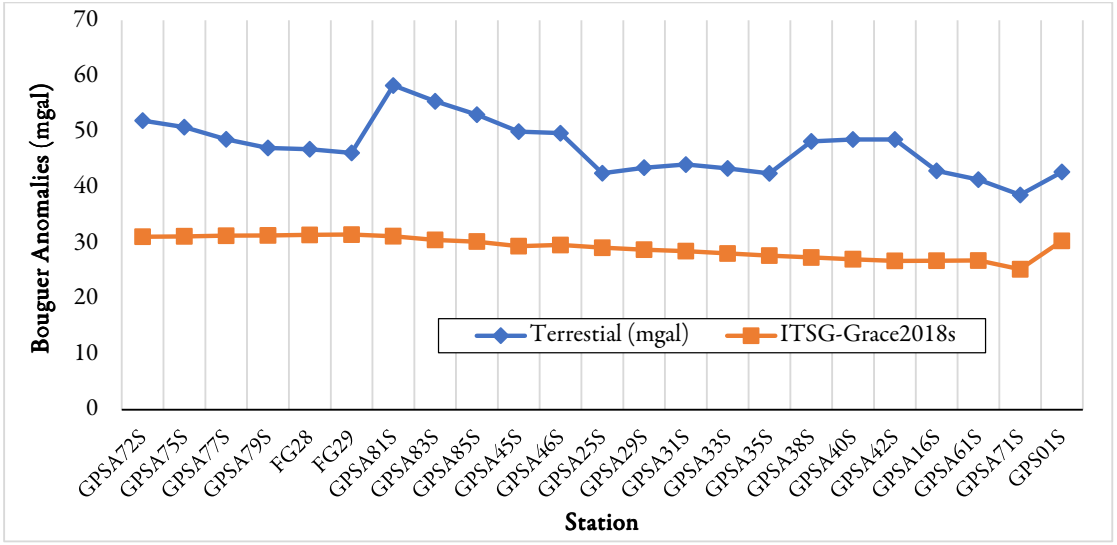

Figure 9. Changes in the terrestrial with ITSG-Grace2018s Free-Air anomaly

It is worth noticing in Figure 9 that the terrestrial (mgal) changes with ITSG-Grace2018s at the rate is 1.45346.

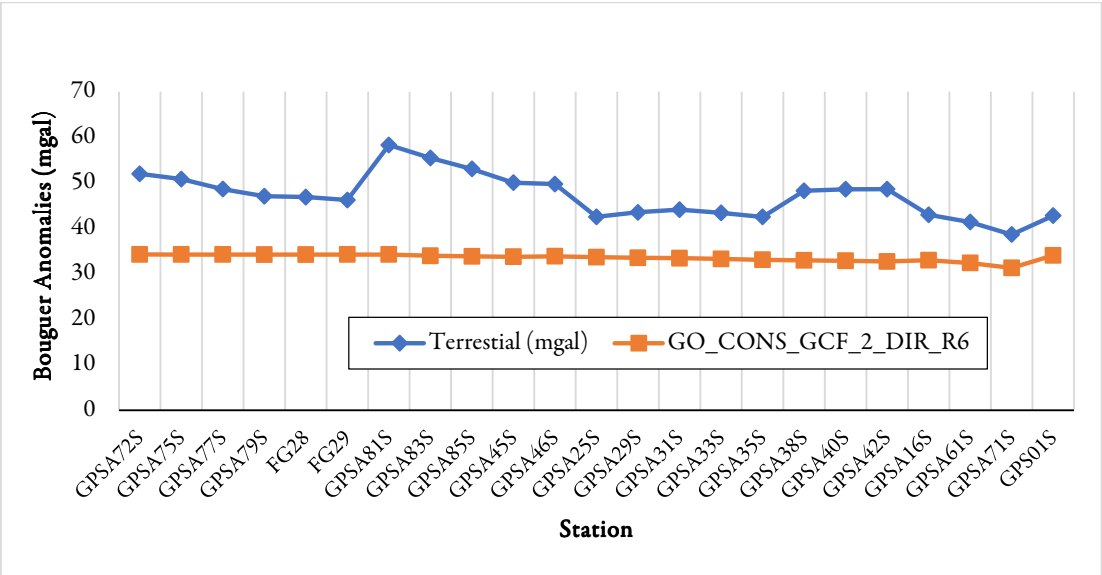

Figure 10. Changes in the terrestrial with go_cons_gcf_2_dir_r6 Free-Air anomaly

The outcome of the linear slope regression through the data points of Terrestrial (mgal) and GO_CONS_GCF_2_DIR_R6 shown in Figure 10 was estimated as 3.710734.

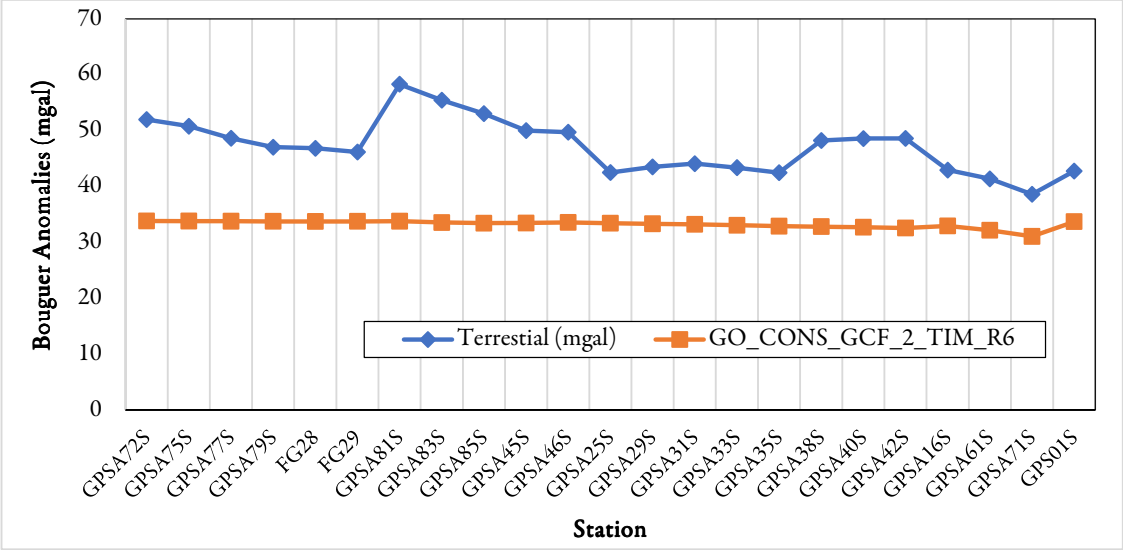

Figure 11. Changes in the terrestrial with go_cons_gcf_2_tim_r6 Free-Air anomaly

It is worth observing in Figure 11 that the changes between the terrestrial (mgal) and GO_CONS_GCF_2_TIM_R6 are 4.09442.

Discussion

EGM2008 and GECO are the two models which are not significantly different from the terrestrial gravity models at 0.01 level of significance as indicated in Table 4. Also, the P-values of these two models are greater than 0.01 level of significance with EGM2008 (0.0393) and GECO (0.0146). T-test suggests that the two models have closer accuracy to the terrestrial observation than the rest of the ten models for Free-Air anomaly data. The closer the value of the correlation coefficient to +/-1, the more accurate the structure of the data of the GGM-derived Free-Air anomaly to the terrestrial Free-Air anomaly while the farther the value of the correlation coefficient from +/-1, the less the accuracy of the data supplied by the GGM-derived anomalies to the terrestrial anomaly at each of the points. From the result, all ten models show a strong positive correlation with the terrestrial data, while SGG_UGM_2 and EGM2008 had correlation values of 0.5995 and 0.5973 respectively, indicating the strongest correlation among the models. This agreed with Peprah *et al.* (2017) that EGM2008 provide a better result and has an agreement with the GPS/Levelling data over the study area, also reaffirmed by Patroba's (2016) assertion that EGM2008 indicate high potential geoid modelling over Kenya. The model with the least value is the EIGEN-GRGS.RL04.MEAN-FIELD with value 0.5420. It is then evident from the result that the SGG_UGM_2 model has the strongest correlation and appears as the most promising model which can be used for Free-Air anomaly modelling of the study area as ascertained by Wei *et al.* (2020) that model SGG-UGM-2 shows promising performance in the GPS/levelling validation.

Conclusion

This research evaluated the accuracy of gravity models (Free-Air) computed from a total of ten (10) Global Gravity Models using terrestrial Free-Air anomalies at a total of twenty-three (23) control points in Akure, Ondo State, Nigeria. The analysis indicates that EGM2008 and GECO models do not significantly differ from terrestrial gravity models at the 0.01 level of significance, with P-values of 0.0393 and 0.0146, respectively. Compared to the other eight models assessed for Free-Air anomaly data. The T-test results show that these two models have closer accuracy to terrestrial observations. All the 10 models have a strong positive correlation with terrestrial data. Among them, SGG_UGM_2 and EGM2008 demonstrate the highest correlation values of 0.5995 and 0.5973, respectively. Equally, the EIGEN-GRGS.RL04.MEAN-FIELD model shows the lowest correlation value at 0.5420. Hence, SGG_UGM_2 appears as the most promising model for Free-Air anomaly modelling in the study area.

The study recommends that more research be done on a similar study in various geographical areas of Nigeria and other nations. Furthermore, temporal analysis can be used to observe how these models' accuracy varies over time. Finally, a study can examine how artificial intelligence and machine learning can be used in improving the precision of these models, especially the most preferred by this research.

Acknowledgements

The author wishes to extend his sincere gratitude to Mr Paul Oloyede for his time taken to download the data and the materials and to the International Centre for Global Earth Models (ICGEM) for providing the Data used for the research.

Conflict of Interests

The author declares that there are no conflicts of interest related to this article.

References

Adefisan EA, Adefowope ED, Okonma FC (2018). Geospatial Assessment of the Coastal Region of Southwest Nigeria. Global Scientific Journal 6(6):133-153.

Apeh OI, Moka EC, Uzodinma VN (2018). Evaluation of gravity data derived from global gravity field models using terrestrial gravity data in Enugu State, Nigeria. Journal of Geodetic Science 8(1):145-153. *https://doi.org/10.1515/jogs-2018-0015*

Apeh OI, Tenzer R (2022). Development of tailored gravity model based on global gravitational and topographic models and terrestrial gravity data for geophysical exploration of southern Benue trough in southeast Nigeria. Journal of Applied Geophysics 198:104561. *https://doi.org/10.1016/j.jappgeo.2022.104561*

Barthelmes F (2013). Definition of functionals of the geopotential and their calculation from spherical harmonic models theory and formulas used by the calculation service of the International Centre for Global Earth Models (ICGEM). Scientific Technical Report STR09/02, Revised Edition, January 2013. *http://icgem.gfz-potsdam.de/ICGEM/*

Barthelmes F (2014). Global models. In: Grafarend E (Ed). Encyclopedia of Geodesy. Springer International Publishing, Switzerland, pp 1-9. *https://doi.org/10.1007/978-3-319-02370-0_43-2*

Brockmann JM, Zehentner N, Höck E, Pail R, Loth I, Mayer-Gürr T, Schuh WD (2014). EGM_TIM_RL05: An independent geoid with centimetre accuracy purely based on the GOCE mission. Geophysical Research Letters 41(22):8089-8099. *https://doi.org/10.1002/2014GL061904*

Featherstone WE, Dentith MC (1997). A geodetic approach to gravity data reduction for geophysics. Computers & Geosciences 23(10):1063-1070. *https://doi.org/10.1016/S0098-3004(97)00092-7*

Gilardoni M, Reguzzoni M, Sampietro D (2016). GECO: a global gravity model by locally combining GOCE data and EGM2008. Studia Geophysica et Geodaetica 60:228-247. *https://doi.org/10.1007/s11200-015-1114-4*

Hackney RI, Featherstone WE (2003). Geophysical perspectives of the 'Gravity Anomaly'. Geophysical Journal International 154(1):35-43. *https://doi.org/10.1046/j.1365-246X.2003.01941.x*

Kvas A, Behzad Pour S, Ellmer M, Klinger B, Strasser S, Zehentner N, Mayer-Gürr T (2019). ITSG-Grace 2018: Overview and evaluation of a new GRACE-only gravity field time series. Journal of Geophysical Research: Solid Earth 124:9332-9344. *https://doi.org/10.1029/2019JB017415*

Liang W, Li J, Xu X, Zhang S, Zhao Y (2020). A High-Resolution Earth's Gravity Field Model SGG-UGM-2 from GOCE, GRACE, Satellite Altimetry, and EGM2008. Engineering 6:860-878. *https://doi.org/10.1016/j.eng.2020.05.008*

Mayer-Gürr T, Zehentner N, Strasser S, Behzadpour S, Kvas A, Klinger B, Ellmer M (2018). ITSG-Grace2018: The new GRACE time series from TU Graz. AGU Fall Meeting.

McKenzie DP (1967). Some remarks on heat flow and gravity anomalies. Journal of Geophysical Research 72(24):6261-6273.

NPC (2007). National Population Commission. Report of Nigeria's National Population Commission on the 2006 Census. (2007). Population and Development Review 33(1):206-210. *http://www.jstor.org/stable/25434601*

Olugbamila OB (2018). Spatial distribution and accessibility to healthcare facilities in Akure South local government area of Ondo State, Nigeria. Analele Universității din Oradea, Seria Geografie 28(1):7-18.

Olujide HM, Amoo NB, Oguntayo SM, Aroge SK, Amoo AO (2018). Geospatial analysis of land use and land cover dynamics in Akure, Nigeria. Dutse Journal of Pure and Applied Sciences 4(1):379-393.

Patroba AO (2016). Assessment of EGM2008 using GPS/levelling and Free-Air gravity anomalies over Nairobi County and its environs. South African Journal of Geomatics 5(1):17-30. *http://dx.doi.org/10.4314/sajg.v5i1.2*

Pavlis NK, Holmes SA, Kenyon SC, Factor JK (2012). The development and evaluation of the Earth Gravitational Model 2008 (EGM2008). Journal of Geophysical Research: Solid Earth 117(B4). *https://doi.org/10.1029/2011JB008916*

Peprah MS, Ziggah YY, Yakubu I (2017). Performance evaluation of the Earth Gravitational Model 2008 (EGM2008) – A case study. South African Journal of Geomatics 6(1):47-72. *http://dx.doi.org/10.4314/sajg.v6i1.4*

Rummel R, Balmino G, Johannessen J, Visser P, Woodworth P (2002). Dedicated gravity field missions – principles and aims. Journal of Geodynamics 33(1-2):3-20. *https://doi.org/10.1016/S0264-3707(01)00050-3*

Tata H, Ono MN (2018). A gravimetric approach for the determination of orthometric heights in Akure environs, Ondo State, Nigeria. Journal of Environment and Earth Science 8(8):75-80.

Usman VA, Makinde EO, Salami AT (2018). Geospatial assessment of the impact of urban sprawl in Akure, southwestern Nigeria. Journal of Geoscience and Environment Protection 6(4):123-140. *https://doi.org/10.4236/gep.2018.64008*

Yilmaz M, Kozlu B (2018). The comparison of gravity anomalies based on recent high-degree global models. Afyon Kocatepe Üniversitesi Fen Ve Mühendislik Bilimleri Dergisi 18(3):981-990. *http://dx.doi.org/10.5578/fmbd.67502*

Yilmaz M, Turgut B, Güllü M, Yilmaz İ (2017). The evaluation of high-degree geopotential models for regional geoid determination in Turkey. Afyon Kocatepe Üniversitesi Fen Ve Mühendislik Bilimleri Dergisi 17(1):147-153.

Yilmaz M, Yilmaz I, Uysal M (2018). The evaluation of gravity anomalies based on global models by land gravity data. International Journal of Geological and Environmental Engineering 12(11):814-820.

Zingerle P, Pail R, Scheinert M, Schaller T (2019). Evaluation of terrestrial and airborne gravity data over Antarctica – A generic approach. Journal of Geodetic Science 9(1):29-40. *https://doi.org/10.1515/jogs-2019-0004*